ACS SENSORS

Article

pubs.acs.org/acssensors

Diagnosis of Tuberculosis Using Colorimetric Gold Nanoparticles on a Paper-Based Analytical Device

Tsung-Ting Tsai,[†,#] Chia-Yu Huang,[‡,#] Chung-An Chen,[‡] Shu-Wei Shen,[‡] Mei-Chia Wang,[§] Chao-Min Cheng,[∥] and Chien-Fu Chen[*,‡]

[†]Department of Orthopaedic Surgery, Bone and Joint Research Center, Chang Gung Memorial Hospital and Chang Gung University College of Medicine, Taoyuan 333, Taiwan

[‡]Institute of Applied Mechanics, National Taiwan University, Taipei 106, Taiwan

[§]Department of Laboratory Medicine, Chang Gung Memorial Hospital, Taoyuan 333, Taiwan

[∥]Institute of Biomedical Engineering, National Tsing Hua University, Hsinchu 300, Taiwan

S *Supporting Information*

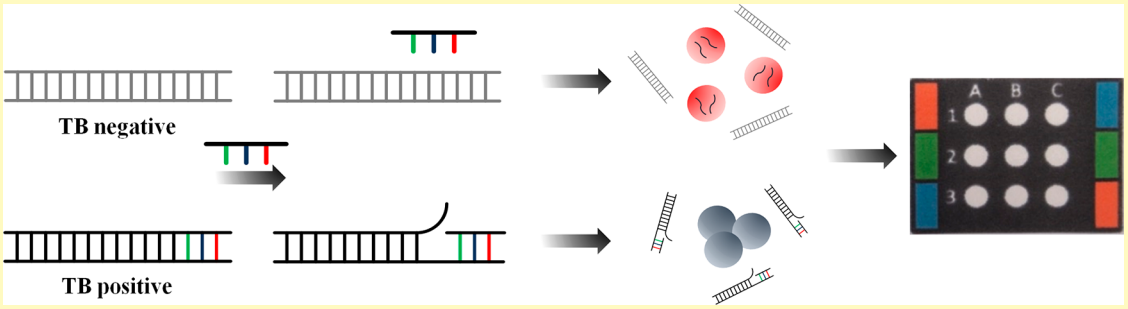

ABSTRACT: We have developed a colorimetric sensing strategy employing gold nanoparticles and a paper-based analytical platform for the diagnosis of tuberculosis (TB). By utilizing the surface plasmon resonance effect, we were able to monitor changes in the color of a gold nanoparticle colloid based on the effects of single-stranded DNA probe molecules hybridizing with targeted double-stranded TB DNA. The hybridization event changes the surface charge density of the nanoparticles, causing them to aggregate to various degrees, which modifies the color of the solution in a manner that can be readily measured to determine the concentration of the targeted DNA analyte. In order to adapt this TB diagnosis method to resource-limited settings, we extended this label-free oligonucleotide and unmodified gold nanoparticle solution-based technique to a paper-based system that can be measured using a smartphone to obtain rapid parallel colorimetric results with low reagent consumption and without the need for sophisticated analytical equipment. In this study, we investigated various assay conditions, including the denaturing temperature and time, different oligonucleotide probe sequences, as well as the ratio of single stranded probe and double stranded target DNA. After optimizing these variables, we were able to achieve a detection limit of 1.95×10^{-2} ng/mL for TB DNA. Furthermore, multiple tests could be performed simultaneously with a 60 min turnaround time.

KEYWORDS: *biosensor, tuberculosis diagnosis, gold nanoparticles, colorimetric assay, paper-based analytical device*

Tuberculosis (TB) is a lethal infectious disease caused by the bacteria *Mycobacterium tuberculosis*. It typically affects the lungs as pulmonary TB, but it can also cause severe meningitis and extrapulmonary infections, such as disseminated acute TB, as well as abdominal, spinal, and pericardial versions of the illness.[1,2] In 2015, the World Health Organization reported that there were approximately 10.4 million new cases of TB in the world, and nearly 1.4 million people had died from the disease that year.[1] When TB occurs in combination with other serious infections, such as HIV, it can complicate what are otherwise effective forms of therapy.[3,4]

For all of these reasons, it is important to develop new methods of TB diagnosis in order to both prevent and treat this illness. Ideally, the test should be sensitive, accurate, and built on an analytical platform that is easy to use and cost-effective. Currently, doctors can diagnose TB in several ways, including sputum smear microscopy,[5−7] immunological methods,[8,9] rapid molecular tests,[10−13] culture-based techniques,[14] as well as with the use of chest X-rays[15] and CT scans.[16] Among these diagnostic methods, certain molecular tests stand out, such as the polymerase chain reaction (PCR) and real-time PCR, which feature both high sensitivity and accuracy of approximately 92−95%. These techniques are also rapid, as the detection process from sampling to result readout can be completed in just 2 h.[13,17] However, the cost for one PCR test is still not affordable enough to serve as a broad screening method in developing

Received: July 3, 2017
Accepted: August 25, 2017
Published: September 13, 2017

DOI: 10.1021/acssensors.7b00450
ACS Sens. 2017, 2, 1345−1354

countries, and the bulky equipment and power requirements also limit the portability of the system. As a result, there is still a need for a rapid, high sensitivity, and cost-effective TB test.

Researchers have developed versatile approaches to disease diagnostics in resource-limited settings. Among the variety of different sensing mechanisms, colorimetric assays based on binary or quasi-quantitative results that can be seen with the naked eye are particularly suitable strategies to pursue.[18] At the same time, as advances in nanotechnology have become more widely available, researchers have been able to develop versatile biochemical sensors based on the extraordinary optophysical and chemical characteristics of these materials for more sensitive, specific, and rapid analysis.[19,20] Among these nanomaterials, gold nanoparticles have been widely adopted as colorimetric sensors to provide alternative schemes to conventional biochemical sensing. Gold nanoparticles are relatively simple to synthesize and use for rapid analysis, as they feature unique optoelectronic and chemical properties, as well as excellent biocompatibility and stability.[21]

One of the most important optical features of gold nanoparticles is surface plasmon resonance, which is related to the nanoparticle's size, shape, composition, and interparticle distance, in addition to the dielectric constant (i.e., refractive index) of the solution.[22] One way that colorimetric sensing using gold nanoparticles can be achieved is by inducing aggregation of the colloid.[23] When the distance between nearby gold nanoparticles decreases, the material's surface plasmon resonance red shifts, causing the color of the suspension to change from wine red to blue.[24] The color change of the AuNP mixture provides a practical platform for absorption-based colorimetric sensing of a target analyte that directly or indirectly triggers AuNP aggregation or redispersion. Mirkin and co-workers first established a DNA biosensor using gold nanoparticles modified with polynucleotides and monitored visible color changes in the nanoparticle solution based on the concentration of the target molecule, which featured complementary base-pairing.[25] The color change could be observed using a UV−vis spectrophotometer or even by just the naked eye. The surface of gold nanoparticles can also be modified with different functionalities to provide highly sensitive and specific detection of a wide range of targets, such as heavy metals,[26−29] various chemical compounds,[30−32] DNA,[33−35] RNA,[36,37] proteins,[38−40] and cells,[41,42] constituting a major achievement in bioanalytical technology.[43]

In this study, we investigated a colorimetric sensing strategy using the surface plasmon resonance of gold nanoparticles for TB diagnosis. Fluorescent label-free, single-stranded oligonucleotide sequences (ssDNA) that targeted double-stranded *M. tuberculosis* DNA (dsDNA, IS6110insertion sequence) were combined in solution with gold nanoparticles. The adsorption of these ssDNA sequences to the gold changes the surface charge density of the nanoparticles, resulting in aggregation of the colloid and affecting the surface plasmon resonance, which manifests as a distinct color change that can be measured using a spectrophotometer. When target TB dsDNA is combined with the probe ssDNA, subsequent hybridization affects the zeta potential of the nanoparticles, and thus by spectroscopically monitoring the degree of color change in the solution, we are able to detect the presence of TB causing bacteria. The size of the AuNPs used in this study was 13 nm in diameter based on the low radiative losses of these materials and the easily overcome surface charge repulsion between neighboring AuNPs to enable aggregation in low concentration solutions of analyte.

To further advance this method of TB diagnosis for resource-limited settings, we incorporated the oligonucleotide sequences and gold nanoparticles into a paper-based (i.e., cellulose) device that could be easily disseminated and used throughout the developing world. Paper devices have been developed for biomedical sensing and analysis in resource limited settings due to their cost effectiveness, disposability, simple fabrication, low sample volume requirements, wettability, and ease of storage and transport.[44−46] In this study, we spotted the gold nanoparticle-ssDNA/dsDNA colloid onto the paper device and then determined the blue/red ratio of each testing spot from the RGB values of a smartphone image, which we correlated with the different degrees of gold nanoparticle aggregation as a function of the increased concentration of the TB target sequences. The use of a smartphone for sample detection enabled us to achieve rapid on-site quantitative and parallel analysis, in addition to providing simple means of data storage via cloud computing, thus requiring minimal equipment.[47] Additionally, only microliters of TB sample were required for the paper test, which is another advantage compared to solution-based methods with shorter response time.

To achieve a low detection limit, we optimized different variables, such as heating temperature, denaturing time, the ratio of ssDNA and TB dsDNA, and different ssDNA probes sequences and length. Additionally, we confirmed the practicability and sensitivity of our gold nanoparticle diagnostic system by testing a real TB patient and comparing the results with established methods of staining and gel electrophoresis of the clinically extracted sample. Therefore, with just a smartphone, from this paper TB test we were able to rapidly measure parallel colorimetric results, eliminating the need for expensive reagents or sophisticated analytical instruments, which suggests this sensitive diagnostic test could have practical value around the world.

EXPERIMENTAL SECTION

Reagents and Materials. All reagents, including methanol (99%), 2-propanol (99%), ethanol (99%), and trisodium citrate (>99%), were purchased from Sigma-Aldrich (St. Louis, MO) unless otherwise stated. Hydrogen tetrachloroaurate (III) trihydrate ($HAuCl_4 \cdot 3H_2O$, 99%) was purchased from Acros Organics (Geel, Belgium). Oligonucleotides were synthesized and purified by Bio Basic Inc. (Ontario, Canada). Ultrapure water (18.2 mΩ·cm) was used throughout the experiments, which was filtered through a Milli-Q system (Millipore, Milford, MA). The QIAamp DNA Mini Kit, Q solution, RNase, and HotStar Taq DNA Polymerase materials were purchased from Qiagen (Hilden, Germany). A High Pure Viral Nucleic Acid Kit was purchased from Roche Applied Science (Mannheim, Germany). AxyPrep Maxi Plasmid Kit was purchased from Axygen Biosciences (Union City, CA). Agarose I and tris-borate-EDTA (TBE) buffer were purchased from Amresco (Solon, OH). Novel Juice was purchased from GeneDirex Inc. (Las Vegas City, NV). Whatman grade 3MM cellulose chromatography paper was purchased from GE Healthcare (Little Chalfont, UK).

Instrumentation. PCR amplification was performed using an Applied Biosystems 2720 Thermal Cycler (Life Technologies, Carlsbad, CA). Transmission electron microscopy (TEM, H7500, Hitachi High-Technologies, Tokyo, Japan) was used to verify the size and morphology of the gold nanoparticles. A UV−vis spectrophotometer (Cintra 10e, GBC, Victoria, Australia) was used to obtain the extinction spectra of the gold nanoparticle colloid to determine the solution concentration and dispersion/aggregation characteristics.

DOI: 10.1021/acssensors.7b00450
ACS Sens. 2017, 2, 1345−1354

Colorimetric results of the paper-based TB test were recorded using a smartphone (iPhone, Apple, CA) under artificial white light without flash and a USB digital microscope (UPG650, Upmost, Taiwan). All data points feature the average and standard deviation of 5 replicate measurements.

Fabrication of the Paper TB Diagnostic Platform. The paper-based devices were made on cellulose paper using a printer (Xerox 8570, Fuji, Japan) and solid wax to print circular 3-mm-diameter hydrophobic barriers on the surface of the paper, which was then heated to 160 °C for 2 min to help the wax penetrate the cellulose fibers to form the testing spots.

After color development, 200 μL of the sample solution was spotted at the center of the hydrophilic circles. A Kimwipe was fixed beneath the paper device using tape to help the device dry more rapidly. When the spotted solution had completely dried, an image of the device was taken using a smartphone under artificial white light without a flash. The RGB values of the image were analyzed using ImageJ software (National Institutes of Health, Bethesda, MD).

Preparation of TB Negative and TB dsDNA Sequences. *Institutional Review Board Approval.* Human disc tissue samples used in this work were approved and issued by the institutional review board of Chang Gung Memorial Hospital, Taoyuan, Taiwan.

TB Negative dsDNA Sequence. As a control, we collected disc tissue samples that were TB negative from patients who had received spinal surgery at Chang Gung Memorial Hospital. The harvested tissues were cut and placed into a tube with 180 μL Buffer ATL and 20 μL Proteinase K (600 mAU/ml) from the QIAamp DNA Mini Kit. TB negative DNA was then extracted using the High Pure Viral Nucleic Acid Kit according to the manufacturer's instructions. The extracted DNA was stored at −80 °C until further use.

TB dsDNA Sequence. The Department of Laboratory Medicine at Chang Gung Memorial Hospital provided the *E. coli* strain TOP10, which had been transformed by the pCR2-TOPO plasmid with the 123 bp IS6110 fragment (i.e., the target TB dsDNA sequence). The bacterial strain was streaked on an LB plate and subcultured in LB medium supplemented with 50 μL of 20 mg/mL ampicillin at 37 °C overnight. The plasmid DNA was extracted from the culture pellet using the AxyPrep Maxi Plasmid Kit, followed by IS6110 PCR to confirm the presence of the 123 bp fragment. The IS6110 primer sequences were 5′-CCTGCGAGCGTAGGCGTCGG-3′ and 5′-CTCGTCCAGCGCCGCTTCGG-3′. 10 μL of DNA template was used in a 50 μL reaction mixture made from the HotStar Taq DNA Polymerase materials, which contained 0.6 μL of 25 μM primer, 4 μL of 2.5 mM dNTP, 5 μL of 5× Q-solution, 5 μL of 10× buffer, 0.25 μL of 5 U/μL HotStar Taq, and 24.55 μL of RNase-free H_2O. PCR amplification was performed with the following temperature cycling conditions: initial denaturation at 94 °C for 15 min, 35 cycles of 94 °C for 1 min, 68 °C for 1 min, 72 °C for 1 min, and a final extension of 72 °C for 10 min. The amplified products were analyzed by gel electrophoresis in 2% agarose prepared in TBE buffer. Finally, Novel Juice was added to the samples, mixed and then loaded on the gel and visualized on a UV transilluminator.

Preparation of Gold Nanoparticles. Briefly, a 25 mL solution containing 38.8 mM trisodium citrate was added to 250 mL of a boiling 1 mM $HAuCl_4$ solution.[21] After continuously heating and stirring for 15 min, the color of the colloid changed from light yellow to wine red, indicating the formation of gold nanoparticles. We then cooled the gold nanoparticle colloid to room temperature. TEM analysis confirmed that the synthesized nanoparticles had a diameter of 13 ± 1 nm. The concentration of the colloid was estimated according to the Beer−Lambert law from the absorption spectrum.

Evaluation of the ssDNA Probe. We designed different ssDNA probes to determine which was the most effective for TB diagnosis. All the probes are listed in Table 1. Briefly, ssDNA sensing probes and TB dsDNA sequences were mixed at a ratio of 1:2 (26 μL of 0.13 nM ssDNA and 87 μL of 0.26 nM target TB dsDNA). The solution was then heated at 95 °C for 180 s in a dry bath. After heating, the mixture was then annealed at 50 °C for 2 min in an incubator and then allowed to rest at room temperature to cool down. 887 μL of the gold nanoparticle colloid (0.5 nM) was then added to this solution, rested for 30 min, and mixed with 0.1 M NaCl solution to induce the aggregation-dependent color change. Finally, the solution was measured using either a UV−vis spectrophotometer or our paper-based detection system.

Table 1. Sequences of the Probe ssDNA for TB Analysis

primer name	sequence
RF15	5′-CCG AAG CGG CGC TGG-3′
RF20	5′-CCG AAG CGG CGC TGG ACG AG-3′
F15S10	5′-GCC GCT TCG GAC CAC-3′
F20S10	5′-GCC GCT TCG GAC CAC CAG CA-3′
RMU	5′-GGACCCGTCCCAAGCGGATG-3′
E20	5′-CCG ACG CCT ACG CTC GCA GG-3′
LMR	5′-CCTAACCGGCTGTGGGTAGC-3′
F25	5′-GTG GTC CGA AGC GGC GCT GGA CGA G-3′
F30	5′-TGC TGG TGG TCC GAA GCG GCG CTG GAC GAG-3′

Determining the Optimal Denaturing Temperature, Time, and Ratio of the Target TB dsDNA Sequences for Hybridization with the Gold Nanoparticles. 26 μL of 0.13 nM ssDNA probe RF15 (Table 1) was mixed with 87 μL of the 0.26 nM target TB dsDNA solution (corresponding to a ratio of 1:2), and then incubated in a dry bath. We tested various denaturing temperatures (85 °C, 90 °C, and 95 °C for 180 s), times (30, 60, 120, 180, 240, 360, or 600 s at 95 °C), and ratios of the ssDNA sensing probe to the targeted TB dsDNA sequence (1:5, 1:3, 1:2, 1:1, 2:1, 3:1, and 5:1 at 95 °C for 180 s). After heating, the samples were annealed at 50 °C for 2 min in the incubator, and then cooled to room temperature. 887 μL of the gold nanoparticle colloid (0.5 nM) was then added to these solutions, rested for 30 min, and then mixed with 0.1 M NaCl solution to induce the color change. Finally, the solution was measured using a UV−vis spectrophotometer or our paper-based detection system. To collect quantitative results, for the solution-based experiments we plotted the 610 nm/520 nm absorption ratio from the spectrophotometric data, and for the paper-based device, we determined the blue to red ratio (B/R) from the red-green-blue (RGB) values of the images taken of the paper tests using a smartphone and ImageJ software.[48]

Paper-Based Colorimetric Diagnosis of TB. For the paper-based test, we used the optimized parameters (i.e., the denaturing temperature and time, ssDNA to dsDNA ratio, and ssDNA sequence) that we determined in the prior experiments. To test a clinical sample, we used a confirmed TB dsDNA sequence provided by the Department of Laboratory Medicine at Chang Gung Memorial Hospital, which had been amplified using PCR. ssDNA sensing probes and TB negative or TB dsDNA sequences (IS6110 sequence, 123 bp fragment) were mixed together (26 μL of 0.13 nM ssDNA and 87 μL of dsDNA). The solution was then heated at 95 °C for 180 s in a dry bath. After heating, the mixture was then annealed at 50 °C for 2 min in an incubator and then allowed to rest at room temperature to cool down. 887 μL of the gold nanoparticle colloid (0.5 nM) was then added to this solution, rested for 30 min, and mixed with 0.1 M NaCl solution to induce the aggregation-dependent color change. Finally, the solution was measured via a UV−vis spectrophotometer or our paper-based detection system.

RESULTS AND DISCUSSION

We synthesized the unmodified gold nanoparticles using the citrate reduction method and determined that the peak absorbance wavelength was centered at 520 nm. The color of the colloid solution was visibly red.[49] When we added NaCl to the colloid, the dissociative ions shielding the negatively charged surface of the gold nanoparticles caused the solution to change in color from red to blue as the nanoparticles became more aggregated.[50]

In a previous study, ssDNA was shown to attach to gold nanoparticle surfaces via hydrophobic interactions, exposing the

DOI: 10.1021/acssensors.7b00450
ACS Sens. 2017, 2, 1345−1354

Scheme 1. Schematic Illustration of the Proposed TB Diagnostic Method

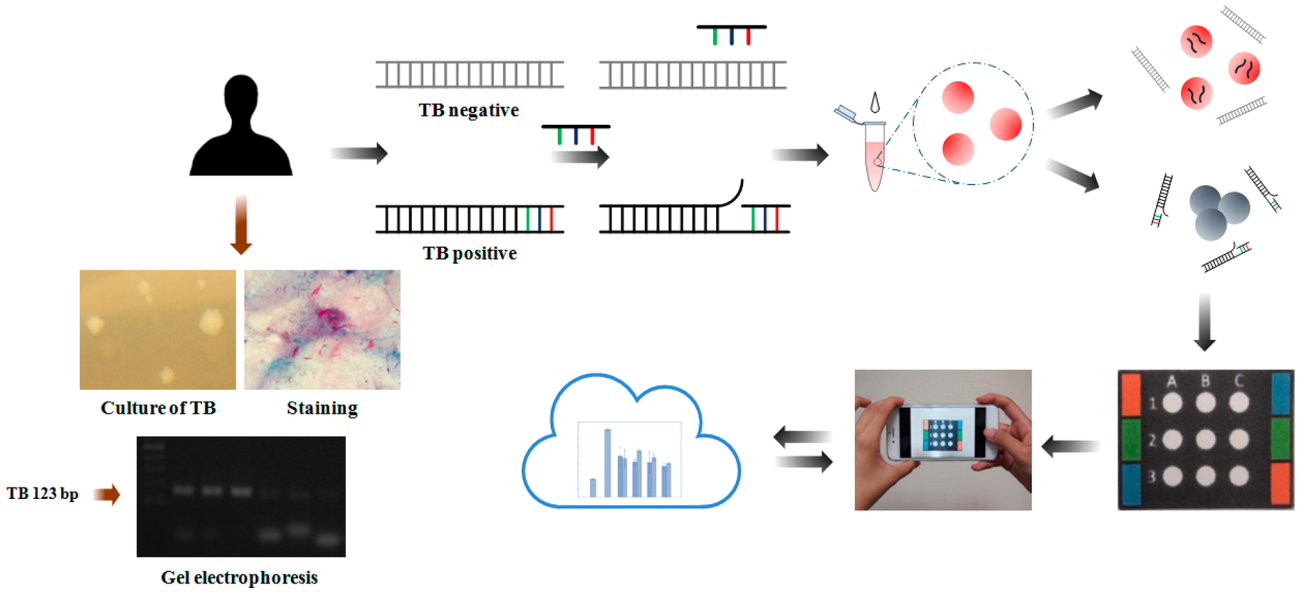

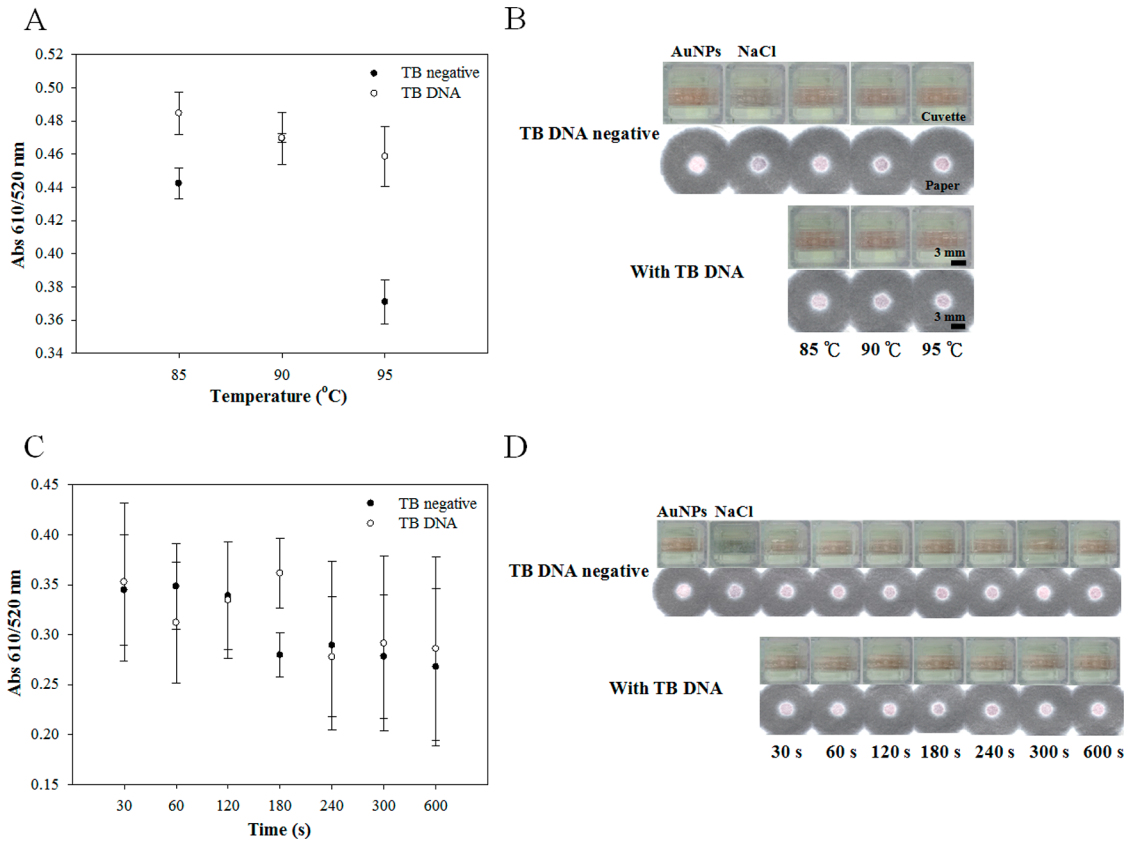

Figure 1. Effects of heating temperature and denaturing time on DNA hybridization for the solution- and paper-based diagnostic platforms. The colorimetric results of TB diagnosis in (A) solution and on (B) paper were tested at 85, 90, and 95 °C heating temperatures for 180 s. Different denaturing times ranging from 30 to 600 s at 95 °C were also tested in (C) solution and on (D) paper. The ssDNA sensing probes (RF15) and TB target dsDNA sequences were mixed at a ratio of 1:2. After annealing at 50 °C for 2 min, the AuNP colloid (0.5 nM) was then added to these solutions, rested for 30 min, and mixed with 0.1 M NaCl to induce the aggregation-dependent color change for colorimetric measurement.

negatively charged phosphate groups of the DNA backbone, thus enhancing the nanoparticles' resistance to the ion shielding effect.[51] However, we hypothesized that the addition of the complementary target dsDNA would result in hybridization with the ssDNA probe molecules, causing the formation of a stable double-helix structure that prevents the exposure of negatively charged phosphate groups. As a result, the zeta potential on the gold nanoparticle surfaces and the electrostatic repulsion between adjacent nanoparticles should decrease, causing the materials to aggregate more after the addition of

DOI: 10.1021/acssensors.7b00450
ACS Sens. 2017, 2, 1345−1354

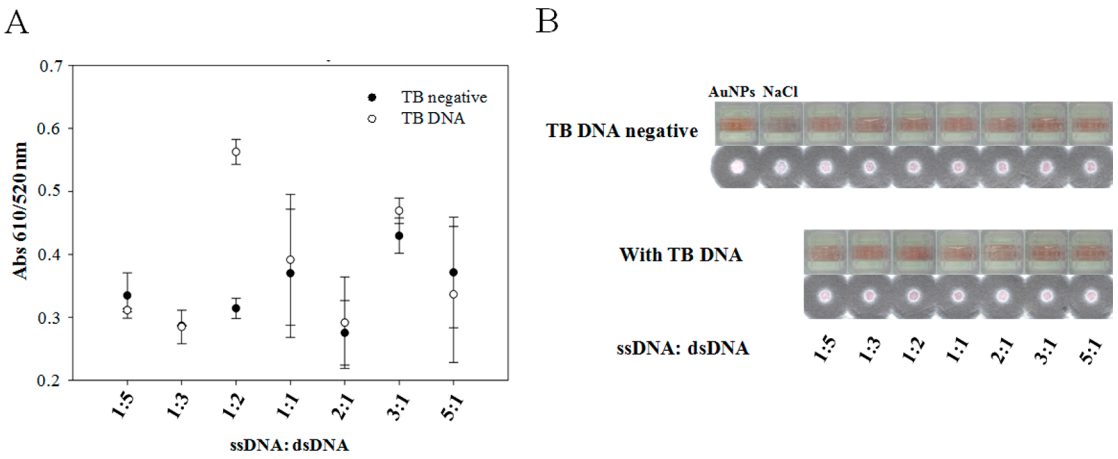

Figure 2. Different ratios of ssDNA probe to target dsDNA sequences for the solution- and paper-based diagnostic platforms. The colorimetric results of TB diagnosis in (A) solution and on (B) paper for ssDNA to dsDNA ratios of 1:5, 1:3, 1:2, 1:1, 2:1, 3:1, and 5:1. The different ratios of ssDNA sensing probes (RF15) and TB target dsDNA sequences were mixed and then heated at 95 °C for 180 s in a dry bath.

NaCl, and thus the extent of color change in the colloid can be used to calculate the amount of TB dsDNA present in solution.

A schematic illustration of the proposed TB diagnosis system is shown in Scheme 1. For all of the experiments, we mixed dsDNA with the detection probe ssDNA sequences, followed by the addition of the gold nanoparticle colloid. If the dsDNA consists of the IS6110 TB target sequence (extracted from a clinical sample), then the ssDNA should hybridize with these strands and the solution color should turn bluer after the addition of NaCl. On the other hand, if the IS6110 TB target sequence is absent from the solution (i.e., TB negative), then the color of the mixture will remain red even after the addition of NaCl.

Effects of Heating Temperature and Denaturing Time on the TB Sensing Platform. Heating temperature and denaturing time are two important factors for increasing the sensitivity and efficiency of DNA biosensors. The heating temperature controls the dissociation of hydrogen bonds between base pairs in the dsDNA sequence, thus converting the material into the single stranded state. Cooling the solution then allows the strands to rehybridize, in this case potentially with the ssDNA probe sequences.

To determine the optimum conditions, we tested three different heating temperatures (85, 90, and 95 °C) for denaturing dsDNA (both TB negative and positive sequences) in the presence of the probe ssDNA, in solution or on paper (Figure 1A,B). Subsequent addition of the gold nanoparticles to the DNA solution followed by NaCl resulted in the colorimetric change from red to purple. Our results showed that the largest color variation resulted from the 95 °C heating temperature (Figure S1). Lowering the heating temperature produced similar absorption results for both the TB negative dsDNA control and the targeted TB dsDNA, but that would lower the sensitivity of the platform. We did not test temperatures greater than 95 °C due to the probability that such conditions may damage the DNA during the denaturing process. Our heating temperature results matched other dsDNA denaturation tests, which have shown that a temperature range of 92−98 °C can effectively separate dsDNA into ssDNA while leaving the DNA structure intact.[52]

We noted that the paper-based method required a much lower sample volume and was faster to measure with a smartphone compared to the solution-based technique, which was limited by the sample requirements and operation speed of the spectrophotometer. Additionally, it was difficult to distinguish the spectrophotometric absorption results at 610 nm for the solution-based method. Overall, we found that the paper-based sensing platform had a greater ability to distinguish the clinical samples (Figures 1 and S1A).

In addition, we also tested the denaturing time from 30 to 600 s in order to identify the optimal condition for dissociation of dsDNA hydrogen bonding to produce ssDNA (Figure 1C−D). The results showed that 180 s denaturing time resulted in the statistically largest color change after the TB ssDNA rehybridized with the ssDNA sensing probes. A shorter denaturing time may result in insufficient dissociation of the targeted TB dsDNA into ssDNA. Alternatively, longer denaturing times may cause the TB dsDNA to completely denature into ssDNA, resulting in an excess amount of ssDNA absorbing on the gold nanoparticles and protecting them from aggregation even after the addition of the salt solution. In fact, we observed lower B/R values for the gold nanoparticle spots on the paper device for longer heating times (Figure S2). As a result, for all subsequent experiments, we used a DNA denaturing temperature and time of 95 °C and 180 s for the detection of TB in this study.

Effect of the Ratio of the Probe ssDNA to the Targeted dsDNA Sequences. In order to obtain a low limit of detection and proper DNA hybridization for the TB sensing platform, it was necessary to determine the ideal ratio of the sensing ssDNA probe sequence to the targeted TB dsDNA. In this sensing platform, we wanted the hybridization of the ssDNA probe sequence to the denatured dsDNA sequence to result in the lowest amount of ssDNA probe molecules to remain suspended in solution, as these materials will attach to gold nanoparticles in order to avoid aggregation after the addition of salt, which will raise the detection limit of the targeted dsDNA sequence. However, if we are able to minimize the amount of ssDNA that remains after the hybridization reaction, the color change will be more significant, increasing the sensitivity and lowering the detection limit. To determine the ideal value, we tested various ratios of ssDNA to dsDNA, including 1:5, 1:3, 1:2, 1:1, 2:1, 3:1, and 5:1 (Figures 2 and S3).

The results showed that when the concentration of the ssDNA probe sequence was equal to or higher than the

DOI: 10.1021/acssensors.7b00450
ACS Sens. 2017, 2, 1345−1354

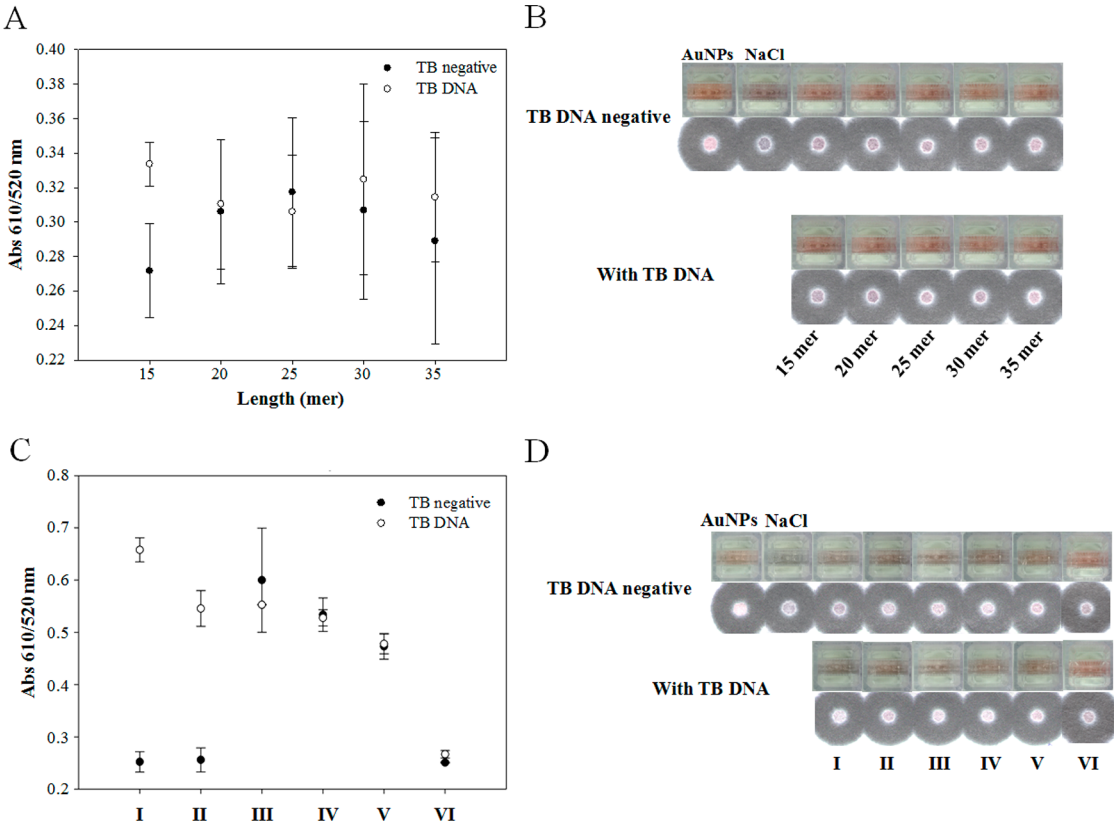

Figure 3. Effect of different oligonucleotide lengths, targeting the IS6110 sequence position, and different oligonucleotide configurations of probe ssDNA sequences for the solution- and paper-based diagnostic platforms. The colorimetric results of the TB diagnosis in (A) solution and on (B) paper for different length oligonucleotide probes, including 15, 20, 25, 30, and 35 mer (named RF15, RF20, F25, F30, and F35, respectively). We also tested different targeting IS6110 sequence positions and oligonucleotide mixtures for the probe ssDNA sequence in (C) solution and on (D) paper. The Roman numerals I–VI represent the sequences of RF15, RF20, F15S10, F20S10, RF20/RMU, and RF20/E20/RMU/LMR, respectively.

targeted dsDNA sequence, the color variance of the gold nanoparticle colloid in both solution and on paper was relatively random, and the samples featuring the TB negative control and TB sequences could not be distinguished. We attributed this result to the remaining ssDNA after rehybridization becoming attached to the gold nanoparticle surfaces, preventing aggregation even after the salt solution had been added. In addition, the excess ssDNA probes may create more dimer and hairpin structures during DNA hybridization, which may disrupt the gold nanoparticle colorimetric results.

Conversely, when the ssDNA to dsDNA ratio was less than 1:2 (i.e., 1:3 and 1:5), the color variance of the gold nanoparticle colloid was limited both in solution and on paper for both the TB negative control and the TB sequences. We attributed this outcome to the fact that the initial amount of the ssDNA probe sequence was too low after hybridization to attach to the gold nanoparticle surfaces, causing no significant difference in the surface charge density of the nanoparticles for either the TB negative control or TB target sequences. Therefore, we determined that a ratio of 1:2 for the ssDNA to dsDNA created the most contrast in the colorimetric results with lower error bars for all the tests (Figure 2a). This ratio also matched the DNA sensing results in another DNA sensing platform.[53] For subsequent tests in this study, we set the concentration of the targeted TB dsDNA to half of the detection limit and used a corresponding 1:2 ratio of probe ssDNA to targeted dsDNA.

Effect of Different ssDNA Probe Sequences and Length. Several TB DNA sequences, such as IS6110 and 16S rDNA, have been demonstrated as effective detection targets from extracted sputum and tissue samples.[54,55] In this study, we chose the IS6110 dsDNA sequence of *M. tuberculosis* as the target for disease recognition in order to more easily compare our detection results to others. We studied 9 different variations of the complementary sequence (i.e., the probe ssDNA), featuring different oligonucleotide lengths and configurations to examine the effects on the colorimetric sensing platform. All the probe ssDNA sequences that we studied are listed in Table 1, and the resulting TB diagnosis color variation in both solution and on paper are shown in Figure 3. Our results demonstrate that the 5′-CCG AAG CGG CGC TGG-3′ (TB RF15) sequence, which had been used in all of the previous experiments, possessed the best specificity and selectivity for the TB target dsDNA sequence of all those studied. The outcome of this experiment appears to have been mainly affected by the length of the sensing oligonucleotide probes. In theory, longer oligonucleotides consisting of more bases should have higher sensitivity and specificity sensing results.[56] However, longer oligonucleotide probes not only have slow hybridization kinetics, but they can also form coil or hairpin structures rather than completely exposing their bases in solution, preventing efficient hybridization.[57] In this study, we tested different lengths of oligonucleotide probes, including 15, 20, 25, 30, and 35mer. Our results showed that the 15mer oligonucleotide probe had the highest specificity and selectivity compared to longer and different mixtures of sequences (Figures S4 and S5). We did not test shorter oligonucleotide

DOI: 10.1021/acssensors.7b00450
ACS Sens. 2017, 2, 1345−1354

probes because we believe this could sacrifice the specificity of the reaction.

In addition, compared to the F15S10 ssDNA sensing probe, the RF15 ssDNA probe has the same length (15 mer) but possesses better performance. This result can be attributed to the lower hairpin melting temperature of the RF15 probe (T_m = 35.1, 36.2, 21.7 °C) compared to F15S10 (T_m = 51.1 °C). In this study, we used 50 °C for DNA hybridization. Therefore, the F15S10 probe was able to form the hairpin conformation more easily, which makes it less able to hybridize with the target TB dsDNA sequences.

Clinical Test Using the Optimized Parameters. In order to verify the capability of the gold nanoparticle paper TB diagnostic platform in a resource limited setting, we compared the colorimetric sensing results fora clinical sample of the IS6110 target dsDNA sequence using the optimized parameters in both solution (Figure 4A) and on paper (Figure 4B). The target dsDNA sequences were extracted from a TB patient by spinal surgery at Chang Gung Memorial Hospital, whose diagnosis had been confirmed with a tissue culture following PCR amplification of the IS6110 specific segment. We also confirmed the purity of the IS6110 dsDNA sequence using gel electrophoresis, and then tested the material using our solution- and paper-based platforms with different concentrations of the TB dsDNA and TB negative sequences (i.e., the blank) to confirm this sensing platform for clinical diagnosis. We calculate the limit of detection of the paper devices using the equation: LOD = y_{blank} + 3SD_{blank}, in which y_{blank} is the average signal intensity of the TB negative sample and SD_{blank} is the standard deviation of the TB negative measurements. In this study, we determined that the detection limit of the paper-based colorimetric sensing platform was 1.95 × 10^{-2} ng/mL (S/N = 3), which based on the equation featured a linear dynamic range from 1.95 × 10^{-2} to 1.95 × 10^{1} ng/mL (Figure 4). These results demonstrate that this colorimetric assay combining gold nanoparticles, ssDNA, a simple paper test strip, and a smartphone can be used for the diagnosis of TB in a highly sensitive and specific manner, which could potentially be used around the world, particularly in developing regions.

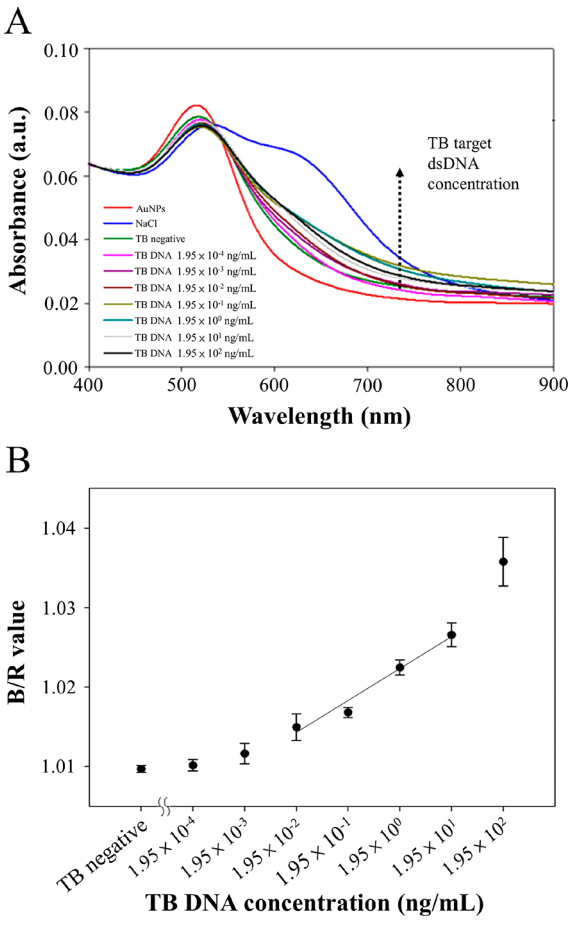

Figure 4. Sensitivity test results of the optimized parameters of the solution- and paper-based TB diagnostic platforms. The colorimetric results of TB diagnosis in (A) solution and on (B) paper were measured for the TB negative sample and different concentrations of the IS6110 target dsDNA sequences from 1.95 × 10^{-4} ng/mL to 1.95 × 10^{2} ng/mL. As a result, the detection limit was 1.95 × 10^{-2} ng/mL, with a linear dynamic range from 1.95 × 10^{-2} to 1.95 × 10^{1} ng/mL (n = 5).

CONCLUSIONS

TB diagnosis remains a great challenge due to the fact that the majority of newly infected cases are in developing countries. Hence, a rapid, simple, low-cost, and accurate on-site detection platform for TB diagnosis is needed to achieve early detection for better infection control and treatment. In this work, we studied a colorimetric sensing strategy utilizing the surface plasmon resonance effect of gold nanoparticles, in which the color of the nanoparticle colloid changes under different aggregation states in the presence of targeted *M. tuberculosis* dsDNA sequences for TB molecular diagnosis.

In order to further extend the capability of TB diagnosis in resource-limited settings, we adapted this method to a simple paper-based platform—the colorimetric results of which can be measured using only a smartphone to obtain rapid parallel readouts with low reagent consumption and without the need for sophisticated analytical equipment.[58] After optimization, we determined our platform has a detection limit for TB dsDNA sequences of 1.95 × 10^{-2} ng/mL, with a linear dynamic range of 1.95 × 10^{-2} to 1.95 × 10^{1} ng/mL. A comparison of different TB detection platforms showed that the sensitivity of the proposed platform is comparable with other detection methods (Table S1).[59−62] We also note that compared to traditional clinical molecular diagnostics that require several hours to complete, the turnaround time for this paper-based sensing platform can be effectively completed in 1 h after DNA extraction.

The low color variance of the paper testing results is mainly caused by the use of low concentration clinical samples and low sample volumes to better simulate point-of-care testing. As a result, the amount of solution used in these images was much less (200 μL) compared to colorimetric tests performed in a cuvette and measured via UV absorbance (>1 mL). However, the colors and the color change of the experimental results can be enhanced by image processing, and this process can be readily automated with a smartphone app for clinical use.

We expect that hundreds of these test results could be analyzed in parallel via an app or cloud computing, with the results being transmitted into the database of a clinical center for disease management and long-term post-therapy monitoring. We have also successfully used the paper-based sensing platform on DNA extracted from infected tissue obtained during surgical operation at a medical center for preliminary TB confirmation. In this study, the target TB dsDNA samples used in each test were individually obtained from the medical center.

DOI: 10.1021/acssensors.7b00450
ACS Sens. 2017, 2, 1345−1354

In addition, none of the clinical dsDNA samples were pretreated prior to the colorimetric tests. Therefore, the amount of salt in each dsDNA solution could dramatically affect the AuNP-based colorimetric results (especially due to the low sample volume and low concentration used in the experimental setup). Proper desalting processes can be adopted to minimize the variance of the samples.

We anticipate that other signal amplification methods, such as biobarcodes or multiple signaling tags, could be further incorporated to lower the detection limit.[63,64] We believe the proposed platform possesses the potential for affordable, sensitive, specific, user-friendly, rapid, and equipment-free diagnostic applications, and anticipate it could be readily translated to the detection of other diseases as well.

■ ASSOCIATED CONTENT

Supporting Information

The Supporting Information is available free of charge on the ACS Publications website at DOI: 10.1021/acssensors.7b00450.

Effects of heating temperature on DNA hybridization; effects of different heating times on DNA denaturation; colorimetric effect of the ratio of the ssDNA probe to dsDNA target sequences; effect of different oligonucleotide lengths and configurations; comparison of different TB detection platforms (PDF)

■ AUTHOR INFORMATION

Corresponding Author

*E-mail: stevechen@ntu.edu.tw.

ORCID

Chien-Fu Chen: 0000-0001-7459-1649

Author Contributions

#Tsung-Ting Tsai and Chia-Yu Huang contributed equally to this work.

Notes

The authors declare no competing financial interest.

■ ACKNOWLEDGMENTS

This research was supported by the Ministry of Science and Technology, Taiwan (MOST 106-2221-E-002-139-MY2, 104-2113-M-005-006-MY2, and 104-2314-B-182-012-MY2), the Chang Gung Memorial Hospital (Linkou) under grant number CMRPG3F1191, and the Aim for Top University Project at National Taiwan University.

■ REFERENCES

(1) WHO, *Global Tuberculosis Report 2016*. 2016.

(2) Shingadia, D.; Novelli, V. Diagnosis and treatment of tuberculosis in children. *Lancet Infect. Dis.* **2003**, *3*, 624−632.

(3) Clouse, K.; Blevins, M.; Lindegren, M. L.; Yotebieng, M.; Nguyen, D. T.; Omondi, A.; Michael, D.; Zannou, D. M.; Carriquiry, G.; Pettit, A. Low implementation of Xpert MTB/RIF among HIV/TB co-infected adults in the International epidemiologic Databases to Evaluate AIDS (IeDEA) program. *PLoS One* **2017**, *12*, e0171384.

(4) Sinshaw, Y.; Alemu, S.; Fekadu, A.; Gizachew, M. Successful TB treatment outcome and its associated factors among TB/HIV co-infected patients attending Gondar University Referral Hospital, Northwest Ethiopia: an institution based cross-sectional study. *BMC Infect. Dis.* **2017**, *17*, 132.

(5) Deka, D. J.; Choudhury, B.; Talukdar, P.; Lo, T. Q.; Das, B.; Nair, S. A.; Moonan, P. K.; Kumar, A. M. What a difference a day makes: same-day vs. 2-day sputum smear microscopy for diagnosing tuberculosis. *Public Health Action* **2016**, *6*, 232−236.

(6) N'Guessan, K.; Horo, K.; Coulibaly, I.; Adegbele, J.; Kouame-Adjei, N.; Seck-Angu, H.; Guei, A.; Kouakou, J.; Dosso, M. Rapid detection of Mycobacterium tuberculosis complex in sputum Samples using PURE TB-LAMP assay. *Int. J. Mycobacteriol* **2016**, *5*, S164−S165.

(7) Ndubuisi, N. O.; Azuonye, O. R.; Victor, N. O.; Robert, O. C.; Vivian, O. Front-loaded sputum microscopy in the diagnosis of pulmonary tuberculosis. *Int. J. Mycobacteriol* **2016**, *5*, 489−492.

(8) Hur, Y. G.; Kang, Y. A.; Jang, S. H.; Hong, J. Y.; Kim, A.; Lee, S. A.; Kim, Y.; Cho, S. N. Adjunctive biomarkers for improving diagnosis of tuberculosis and monitoring therapeutic effects. *J. Infect.* **2015**, *70*, 346−355.

(9) Jacobs, R.; Maasdorp, E.; Malherbe, S.; Loxton, A. G.; Stanley, K.; van der Spuy, G.; Walzl, G.; Chegou, N. N. Diagnostic Potential of Novel Salivary Host Biomarkers as Candidates for the Immunological Diagnosis of Tuberculosis Disease and Monitoring of Tuberculosis Treatment Response. *PLoS One* **2016**, *11*, e0160546.

(10) Mokaddas, E. M.; Saadaldeen, H.; Ahmad, S. Comparison of two molecular methods and an automated liquid culture system for the early detection of Mycobacterium tuberculosis from both pulmonary and extrapulmonary specimens in Kuwait. *Int. J. Mycobacteriol* **2016**, *5*, S74−S75.

(11) Gutierrez, C. Benefits and challenges of molecular diagnostics for childhood tuberculosis. *Int. J. Mycobacteriol* **2016**, *5*, S4−S5.

(12) Yousef, S. A.; AbdelRahim, K. A.; Ahmed, A. O.; Almaary, K. S.; Mohamed, A. M. Diagnosis of Pulmonary Tuberculosis and Detection of Resistance to Rifampin and Isoniazid through Direct Molecular Methods in Stool Samples. *Ann. Clin. Lab. Sci.* **2016**, *46*, 616−621.

(13) Boehme, C. C.; Nabeta, P.; Hillemann, D.; Nicol, M. P.; Shenai, S.; Krapp, F.; Allen, J.; Tahirli, R.; Blakemore, R.; Rustomjee, R.; Milovic, A.; Jones, M.; O'Brien, S. M.; Persing, D. H.; Ruesch-Gerdes, S.; Gotuzzo, E.; Rodrigues, C.; Alland, D.; Perkins, M. D. Rapid Molecular Detection of Tuberculosis and Rifampin Resistance. *N. Engl. J. Med.* **2010**, *363*, 1005−1015.

(14) Ko, Y.; Kim, C.; Chang, B.; Lee, S. Y.; Park, S. Y.; Mo, E. K.; Hong, S. J.; Lee, M. G.; Hyun, I. G.; Park, Y. B. Loculated Tuberculous Pleural Effusion: Easily Identifiable and Clinically Useful Predictor of Positive Mycobacterial Culture from Pleural Fluid. *Tuberc. Respir. Dis (Seoul)* **2017**, *80*, 35−44.

(15) Weinrich, J. M.; Diel, R.; Sauer, M.; Henes, F. O.; Meywald-Walter, K.; Adam, G.; Schon, G.; Bannas, P. Yield of chest X-ray tuberculosis screening of immigrants during the European refugee crisis of 2015: a single-centre experience. *Eur. Radiol.* **2017**, *27*, 3244−3248.

(16) Mehrain, P.; Moghaddam, A. M.; Tavakol, E.; Amini, A.; Moghimi, M.; Kabir, A.; Velayati, A. A. Mediastinal lymphadenopathy in pediatric tuberculosis in computed tomography scan. *Int. J. Mycobacteriol* **2016**, *5*, S242−S243.

(17) Boehme, C. C.; Nabeta, P.; Hillemann, D.; Nicol, M. P.; Shenai, S.; Krapp, F.; Allen, J.; Tahirli, R.; Blakemore, R.; Rustomjee, R. Rapid molecular detection of tuberculosis and rifampin resistance. *N. Engl. J. Med.* **2010**, *363*, 1005−1015.

(18) Qiu, L. P.; Shen, Z. F.; Wu, Z. S.; Shen, G. L.; Yu, R. Q. Discovery of the unique self-assembly behavior of terminal suckers-contained dsDNA onto GNP and novel "light-up" colorimetric assay of nucleic acids. *Biosens. Bioelectron.* **2015**, *64*, 292−299.

(19) Chen, J.; Andler, S. M.; Goddard, J. M.; Nugen, S. R.; Rotello, V. M. Integrating recognition elements with nanomaterials for bacteria sensing. *Chem. Soc. Rev.* **2017**, *46*, 1272−1283.

(20) Chen, Y.; Zhou, S.; Li, L.; Zhu, J.-j. Nanomaterials-based sensitive electrochemiluminescence biosensing. *Nano Today* **2017**, *12*, 98−115.

(21) Saha, K.; Agasti, S. S.; Kim, C.; Li, X. N.; Rotello, V. M. Gold Nanoparticles in Chemical and Biological Sensing. *Chem. Rev.* **2012**, *112*, 2739−2779.

(22) Vilela, D.; Gonzalez, M. C.; Escarpa, A. Sensing colorimetric approaches based on gold and silver nanoparticles aggregation:

DOI: 10.1021/acssensors.7b00450
ACS Sens. 2017, 2, 1345−1354

Chemical creativity behind the assay. A review. *Anal. Chim. Acta* **2012**, *751*, 24−43.
(23) Yuan, Z. Q.; Hu, C. C.; Chang, H. T.; Lu, C. Gold nanoparticles as sensitive optical probes. *Analyst* **2016**, *141*, 1611−1626.
(24) Wang, C. C.; Wu, S. M.; Li, H. W.; Chang, H. T. Biomedical Applications of DNA-Conjugated Gold Nanoparticles. *ChemBioChem* **2016**, *17*, 1052−1062.
(25) Elghanian, R.; Storhoff, J. J.; Mucic, R. C.; Letsinger, R. L.; Mirkin, C. A. Selective colorimetric detection of polynucleotides based on the distance-dependent optical properties of gold nanoparticles. *Science* **1997**, *277*, 1078−1081.
(26) Lin, Y. W.; Huang, C. C.; Chang, H. T. Gold nanoparticle probes for the detection of mercury, lead and copper ions. *Analyst* **2011**, *136*, 863−871.
(27) Zhou, G.; Chang, J.; Pu, H.; Shi, K.; Mao, S.; Sui, X.; Ren, R.; Cui, S.; Chen, J. Ultrasensitive mercury ion detection using dna-functionalized molybdenum disulfide nanosheet/gold nanoparticle hybrid field-effect transistor device. *ACS Sens.* **2016**, *1*, 295−302.
(28) Wang, G. K.; Lu, Y. F.; Yan, C. L.; Lu, Y. DNA-functionalization gold nanoparticles based fluorescence sensor for sensitive detection of Hg2+ in aqueous solution. *Sens. Actuators, B* **2015**, *211*, 1−6.
(29) Tan, L. L.; Chen, Z. B.; Zhao, Y.; Wei, X. C.; Li, Y. H.; Zhang, C.; Wei, X. L.; Hu, X. C. Dual channel sensor for detection and discrimination of heavy metal ions based on colorimetric and fluorescence response of the AuNPs-DNA conjugates. *Biosens. Bioelectron.* **2016**, *85*, 414−421.
(30) Du, L. Y.; Ji, W.; Zhang, Y. F.; Zhang, C. Y.; Liu, G. F.; Wang, S. H. An ultrasensitive detection of 17 beta-estradiol using a gold nanoparticle-based fluorescence immunoassay. *Analyst* **2015**, *140*, 2001−2007.
(31) Song, J.; Wu, F. Y.; Wan, Y. Q.; Ma, L. H. Ultrasensitive turn-on fluorescent detection of trace thiocyanate based on fluorescence resonance energy transfer. *Talanta* **2015**, *132*, 619−624.
(32) Chen, J. H.; Wen, J. L.; Zhuang, L.; Zhou, S. G. An enzyme-free catalytic DNA circuit for amplified detection of aflatoxin B1 using gold nanoparticles as colorimetric indicators. *Nanoscale* **2016**, *8*, 9791−9797.
(33) Sanromán-Iglesias, M.; Lawrie, C. H.; Schäfer, T.; Grzelczak, M.; Liz-Marzán, L. M. Sensitivity Limit of Nanoparticle Biosensors in the Discrimination of Single Nucleotide Polymorphism. *ACS Sens.* **2016**, *1*, 1110−1116.
(34) Ma, L.; Lei, Z.; Liu, X.; Liu, D. J.; Wang, Z. X. Surface ligation-based resonance light scattering analysis of methylated genomic DNA on a microarray platform. *Analyst* **2016**, *141*, 3084−3089.
(35) Hizir, M. S.; Top, M.; Balcioglu, M.; Rana, M.; Robertson, N. M.; Shen, F. S.; Sheng, J.; Yigit, M. V. Multiplexed Activity of perAuxidase: DNA-Capped AuNPs Act as Adjustable Peroxidase. *Anal. Chem.* **2016**, *88*, 600−605.
(36) Joshi, V. G.; Chindera, K.; Singh, A. K.; Sahoo, A. P.; Dighe, V. D.; Thakuria, D.; Tiwari, A. K.; Kumar, S. Rapid label-free visual assay for the detection and quantification of viral RNA using peptide nucleic acid (PNA) and gold nanoparticles (AuNPs). *Anal. Chim. Acta* **2013**, *795*, 1−7.
(37) Wang, Q.; Liu, R. J.; Yang, X. H.; Wang, K. M.; Zhu, J. Q.; He, L. L.; Li, Q. Surface plasmon resonance biosensor for enzyme-free amplified microRNA detection based on gold nanoparticles and DNA supersandwich. *Sens. Actuators, B* **2016**, *223*, 613−620.
(38) Retout, M.; Valkenier, H.; Triffaux, E.; Doneux, T.; Bartik, K.; Bruylants, G. Rapid and Selective Detection of Proteins by Dual Trapping Using Gold Nanoparticles Functionalized with Peptide Aptamers. *ACS Sens.* **2016**, *1*, 929−933.
(39) Lee, J. O.; Kim, E. J.; Lim, B.; Kim, T. W.; Kim, Y. P. Rapid Detection of Protein Phosphatase Activity Using Zn(II)Coordinated Gold Nanosensors Based on His-Tagged Phosphopeptides. *Anal. Chem.* **2015**, *87*, 1257−1265.
(40) Ghasemi, F.; Hormozi-Nezhad, M. R.; Mahmoudi, M. A colorimetric sensor array for detection and discrimination of biothiols based on aggregation of gold nanoparticles. *Anal. Chim. Acta* **2015**, *882*, 58−67.
(41) Ye, X. S.; Shi, H.; He, X. X.; Wang, K. M.; He, D. G.; Yan, L. A.; Xu, F. Z.; Lei, Y. L.; Tang, J. L.; Yu, Y. R. Iodide-Responsive Cu-Au Nanoparticle-Based Colorimetric Platform for Ultrasensitive Detection of Target Cancer Cells. *Anal. Chem.* **2015**, *87*, 7141−7147.
(42) Yang, Y. J.; Huang, J.; Yang, X. H.; Quan, K.; Wang, H.; Ying, L.; Xie, N. L.; Ou, M.; Wang, K. M. Aptazyme-Gold Nanoparticle Sensor for Amplified Molecular Probing in Living Cells. *Anal. Chem.* **2016**, *88*, 5981−5987.
(43) Kim, J. E.; Choi, J. H.; Colas, M.; Kim, D. H.; Lee, H. Gold-based hybrid nanomaterials for biosensing and molecular diagnostic applications. *Biosens. Bioelectron.* **2016**, *80*, 543−559.
(44) Russell, S. M.; Domenech-Sanchez, A.; de la Rica, R. Augmented Reality for Real-Time Detection and Interpretation of Colorimetric Signals Generated by Paper-Based Biosensors. *ACS sens.* **2017**, *2*, 848−853.
(45) Li, B.; Zhang, Z.; Qi, J.; Zhou, N.; Qin, S.; Choo, J.; Chen, L. Quantum Dot-Based Molecularly Imprinted Polymers on Three-Dimensional Origami Paper Microfluidic Chip for Fluorescence Detection of Phycocyanin. *ACS sens.* **2017**, *2*, 243−250.
(46) Chen, G.-H.; Chen, W.-Y.; Yen, Y.-C.; Wang, C.-W.; Chang, H.-T.; Chen, C.-F. Detection of mercury (II) ions using colorimetric gold nanoparticles on paper-based analytical devices. *Anal. Chem.* **2014**, *86*, 6843−6849.
(47) Wu, M. Y.-C.; Hsu, M.-Y.; Chen, S.-J.; Hwang, D.-K.; Yen, T.-H.; Cheng, C.-M. Point-of-Care Detection Devices for Food Safety Monitoring: Proactive Disease Prevention. *Trends Biotechnol.* **2017**, *35*, 288−300.
(48) Chen, G. H.; Chen, W. Y.; Yen, Y. C.; Wang, C. W.; Chang, H. T.; Chen, C. F. Detection of Mercury(II) Ions Using Colorimetric Gold Nanoparticles on Paper-Based Analytical Devices. *Anal. Chem.* **2014**, *86*, 6843−6849.
(49) Storhoff, J. J.; Lazarides, A. A.; Mucic, R. C.; Mirkin, C. A.; Letsinger, R. L.; Schatz, G. C. What controls the optical properties of DNA-linked gold nanoparticle assemblies? *J. Am. Chem. Soc.* **2000**, *122*, 4640−4650.
(50) Zhao, W.; Brook, M. A.; Li, Y. Design of gold nanoparticle-based colorimetric biosensing assays. *ChemBioChem* **2008**, *9*, 2363−2371.
(51) Nelson, E. M.; Rothberg, L. J. Kinetics and mechanism of single-stranded DNA adsorption onto citrate-stabilized gold nanoparticles in colloidal solution. *Langmuir* **2011**, *27*, 1770−1777.
(52) Karni, M.; Zidon, D.; Polak, P.; Zalevsky, Z.; Shefi, O. Thermal Degradation of DNA. *DNA Cell Biol.* **2013**, *32*, 298−301.
(53) Wu, C. K.; Zhou, Y. M.; Miao, X. M.; Ling, L. S. A novel fluorescent biosensor for sequence-specific recognition of double-stranded DNA with the platform of graphene oxide. *Analyst* **2011**, *136*, 2106−2110.
(54) Eisenach, K. D.; Cave, M. D.; Bates, J. H.; Crawford, J. T. Polymerase chain reaction amplification of a repetitive DNA sequence specific for Mycobacterium tuberculosis. *J. Infect. Dis.* **1990**, *161*, 977−981.
(55) Noordhoek, G. T.; Kolk, A.; Bjune, G.; Catty, D.; Dale, J. W.; Fine, P.; Godfrey-Faussett, P.; Cho, S.-N.; Shinnick, T.; Svenson, S. Sensitivity and specificity of PCR for detection of Mycobacterium tuberculosis: a blind comparison study among seven laboratories. *J. Clin. Microbiol.* **1994**, *32*, 277−284.
(56) Williams, A. J.; Pence, H. E. Smart Phones, a Powerful Tool in the Chemistry Classroom. *J. Chem. Educ.* **2011**, *88*, 683−686.
(57) Bonnet, G.; Tyagi, S.; Libchaber, A.; Kramer, F. R. Thermodynamic basis of the enhanced specificity of structured DNA probes. *Proc. Natl. Acad. Sci. U. S. A.* **1999**, *96*, 6171−6176.
(58) Shen, L.; Hagen, J. A.; Papautsky, I. Point-of-care colorimetric detection with a smartphone. *Lab Chip* **2012**, *12*, 4240−4243.
(59) Phunpae, P.; Chanwong, S.; Tayapiwatana, C.; Apiratmateekul, N.; Makeudom, A.; Kasinrerk, W. Rapid diagnosis of tuberculosis by identification of Antigen 85 in mycobacterial culture system. *Diagn. Microbiol. Infect. Dis.* **2014**, *78*, 242−248.
(60) Pavankumar, A. R.; Engstrom, A.; Liu, J.; Herthnek, D.; Nilsson, M. Proficient Detection of Multi-Drug-Resistant Mycobacterium

DOI: 10.1021/acssensors.7b00450
ACS Sens. 2017, 2, 1345−1354

tuberculosis by Padlock Probes and Lateral Flow Nucleic Acid Biosensors. *Anal. Chem.* **2016**, *88*, 4277−4284.
(61) Torati, S. R.; Reddy, V.; Yoon, S. S.; Kim, C. Electrochemical biosensor for Mycobacterium tuberculosis DNA detection based on gold nanotubes array electrode platform. *Biosens. Bioelectron.* **2016**, *78*, 483−488.
(62) Kim, E. J.; Kim, E. B.; Lee, S. W.; Cheon, S. A.; Kim, H. J.; Lee, J.; Lee, M. K.; Ko, S.; Park, T. J. An easy and sensitive sandwich assay for detection of Mycobacterium tuberculosis Ag85B antigen using quantum dots and gold nanorods. *Biosens. Bioelectron.* **2017**, *87*, 150−156.
(63) Chapman, R.; Lin, Y.; Burnapp, M.; Bentham, A.; Hillier, D.; Zabron, A.; Khan, S.; Tyreman, M.; Stevens, M. M. Multivalent nanoparticle networks enable point-of-care detection of human phospholipase-A2 in serum. *ACS Nano* **2015**, *9*, 2565−2573.
(64) Thaxton, C. S.; Elghanian, R.; Thomas, A. D.; Stoeva, S. I.; Lee, J.-S.; Smith, N. D.; Schaeffer, A. J.; Klocker, H.; Horninger, W.; Bartsch, G. Nanoparticle-based bio-barcode assay redefines "undetectable" PSA and biochemical recurrence after radical prostatectomy. *Proc. Natl. Acad. Sci. U. S. A.* **2009**, *106*, 18437−18442.

DOI: 10.1021/acssensors.7b00450
ACS Sens. 2017, 2, 1345−1354